European Journal of Protistology 94 (2024) 126084

Contents lists available at ScienceDirect

European Journal of Protistology

journal homepage: www.elsevier.com/locate/ejop

Research Paper

Description and prevalence of gregarines infecting the amphipod *Gammarus pulex*, in the Water of Leith, Scotland, UK

Kevin McKinley [a,b,d], Anastasios D. Tsaousis [b], Sonja Rückert [c,d,*]

[a] School of Applied Sciences, Edinburgh Napier University, Edinburgh, Scotland, UK
[b] Laboratory of Molecular and Evolutionary Parasitology, RAPID Group, School of Biosciences, University of Kent, Canterbury, Kent, England, UK
[c] Department of Eukaryotic Microbiology, Faculty of Biology, University of Duisburg-Essen, Essen, Germany
[d] Centre for Conservation and Restoration Science, School of Applied Sciences, Edinburgh Napier University, Edinburgh, Scotland, UK

ARTICLE INFO

Keywords:
Gregarine apicomplexa
Cephaloidophora
Freshwater shrimp
Gammarus pulex
Infection levels

ABSTRACT

Gregarines are symbiotic protists that are found in a broad spectrum of invertebrates, including insects, crustaceans, and annelids. Among these the globally distributed amphipod *Gammarus pulex* is one of the earliest recognized hosts for aquatic gregarines and is prevalent among macroinvertebrates in freshwater environments. In this study, samples of *G. pulex* were collected in the Water of Leith river, Scotland, UK. Gregarines were identified using light and scanning electron microscopy as well as standard molecular techniques. We identified three septate eugregarine symbionts—*Heliospora longissima*, *Cephaloidophora gammari*, and the here newly characterized *Cephaloidophora conus* n. sp. (formerly *Cephaloidophora* sp.) associated with *Gammarus pulex* in the Water of Leith. Prevalences for identified gregarine species were calculated and seasonal dynamics of gregarine infections/colonization were analyzed. Prevalences were highest in autumn and spring reaching almost 50 %. While the two *Cephaloidophora* species showed similar colonization patterns, the prevalence of *Heliospora* showed an opposite trend. Identifying gregarine infection/colonization patterns is one step towards better understanding the gregarine–host relationship, as well as possible impacts of the gregarines on their hosts.

1. Introduction

Gregarines are a diverse group of symbiotic protists that infect a wide range of invertebrates, including insects, crustaceans, and annelids (Rueckert et al., 2019). The trophozoites (feeding stages) of these single-celled organisms commonly live inside the host's gut (Wakeman et al., 2014). Although they are generally considered commensals, some gregarines have a significant impact on their host's health and behaviour (Field and Michiels, 2006; Marden and Cobb, 2004). It has been shown that gregarine–host symbiotic relationships can cover a wide spectrum from mutualistic, commensalistic, to parasitic (Rueckert et al., 2019). Effects can vary from altering the host population density, behaviour, survival, and/or physiology (Adamo, 2013; Grabner and Sures, 2019; Kamiya et al., 2014; Zamboni and Lima-Junior, 2015).

One of the oldest established host of aquatic gregarines is the globally distributed amphipod crustacean *Gammarus pulex*, which is among the most prevalent macroinvertebrates found in European freshwater environments. In addition to being a vital component of the food chain (Macneil et al., 1999), *G. pulex* plays a crucial role in breaking down organic matter (Palmia et al., 2019; Vigneron et al., 2015). With its rich content of protein, fats, and amino acids (Köprücü and Özdemir, 2005), *G. pulex* boosts fish feed composition, enhances immune responses, increases stress resistance, and promotes growth performance (Rufchaei et al., 2017). The organism is utilized as an economical substitute for animal protein in the diets of premium fish species (Harlıoğlu and Farhadi, 2018). *Gammarus pulex* is host to various symbionts, including two previously described gregarine species: *Cephaloidophora gammari* (Diesing, 1859) Codreanu-Bălcescu, 1996 and *Heliospora longissima* (von Siebold in von Kölliker, 1848).

Gregarine systematics is in flux, but the traditional organization into three main categories (eugregarines, archigregarines, and neogregarines) is still used (Medina-Durán et al., 2020). The gregarines that infect *G. pulex* are categorized as eugregarines. Eugregarine trophozoite morphology can differ between species (Frolova et al., 2021; Medina-Durán et al., 2020), but in general, they are elongated, with a length ranging from a few micrometers to several millimeters (Rueckert et al., 2015). In septate gregarine trophozoites, the anterior region, called the

* Corresponding author at: Department of Eukaryotic Microbiology, University of Duisburg-Essen, Essen, Germany.
E-mail address: sonja.rueckert@uni-due.de (S. Rückert).

https://doi.org/10.1016/j.ejop.2024.126084

Available online 19 April 2024

protomerite, includes an epimerite—a specialized structure that helps the symbiont to attach to the host's gut epithelium (Valigurová and Florent, 2021). The posterior region of the trophozoite is called the deutomerite, which contains the cell's nucleus (Sokolova et al., 2013). Septate eugregarines are mostly found in the intestines of arthropods (Simdyanov et al., 2017).

In some cases, gregarine symbionts are present in almost all individuals of a given species, while in others, they are rare or absent altogether. For example, a study conducted by Schall (2021) reports that 90 % of earthworms in a particular population were infected with gregarines, while Diakin et al. (2016) described a gregarine infection in only ~ 10 % of amphipods in their study area. One of the main factors that can affect gregarine prevalence for example in odonates is the host's diet (Ilvonen et al., 2018). The prevalence of gregarines can also be influenced by the presence of other parasites or pathogens in the host's gut (Rueckert et al., 2019). There are multiple factors that can result in concurrent infections, for example, variations in host feeding ecology, habitat, and population density significantly impact symbiotic infection rates. Symbionts must overcome or adapt to competition with other symbiotic taxa within the host (Rynkiewicz et al., 2015).

In this study, we investigated three septate eugregarine symbionts that share *G. pulex* as host species. They were identified as *H. longissima*, *C. gammari*, and the here newly described *C. conus* n. sp. (previously *Cephaloidophora* sp.). We addressed the molecular phylogenetic positions of these septate eugregarines using SSU rDNA sequences and analysed the seasonal dynamics of gregarine infections and their possible impact on the *G. pulex* population inhabiting the Water of Leith.

2. Material and methods

2.1. Sample collection and light microscopy

Our study was carried out on original material, collected from the Water of Leith river in Scotland (55°89′60.1″N, –3°30′77.9″W). *Gammarus pulex* were caught using a standard kick sampling procedure (Cheshmedjiev et al., 2011). Samples were taken during a sampling period of 1–2 hrs starting between the times of 9–11 a.m. from the same habitat, between November 2020 and January 2022. *Gammarus pulex* specimens were kept alive in aerated river water until dissection, at which point their wet weight (mg) was measured. After measurements were recorded, *G. pulex* specimens were dissected for gregarines by decapitation and by gently pulling out the gut with fine-tipped forceps under a stereomicroscope (Stemi 2000-C, ZEISS). All dissections were done in physiological NaCl solution (154 mM). The gut material was examined under an inverted microscope (Axio Vert.A1, ZEISS) and gregarines were isolated by micromanipulation and washed three times in physiological NaCl solution (154 mM). For measurements, the software 'ZEN Imaging' in combination with a AxioCam ERc 5 s (ZEISS) and an Axio Vert.A1, ZEISS microscope were used. Trophozoite length was measured from the end of the deutomerite to the tip of the protomerite and the width was measured across the centre of the deutomerite. *Cephaloidophora gammari* was identified morphologically using original measurements, and line-drawings from Goodrich (1949) and Narasimhamurti (1964), as well as photographs from Sorcetti and Di Giovanni (1984). *Heliospora longissima* was identified by both morphological and molecular analyses. Gregarines described as *Cephaloidophora* sp. by Wróblewski et al. (2019), were also identified in *G. pulex* in Scotland and are officially described here as *C. conus* n. sp.

2.2. Scanning electron microscopy

Up to 30 individuals of *C. gammari* and *C. conus* n. sp. were prepared for scanning electron microscopy (SEM). Rueckert et al. (2011) had previously provided SEM micrographs of *Heliospora* c.f. *longissima* and therefore these are not included in this study. Individuals were deposited directly into baskets created using the end of a pipette tip attached to 10 μm polycarbonate membrane filter (Millipore Corp., Billerica, MA), that was submerged in physiological NaCl solution (154 mM) in a 6-well multiwell plate. A piece of Whatman No. 1 filter paper was mounted on the inside lid of the multi-well plate. The Whatman filter paper was saturated with 4 % (w/v) OsO_4 and the lid placed back. The gregarines were fixed by OsO_4 vapours for 30 min in the dark. Ten drops of 4 % (w/v) OsO_4 were added directly to the physiological NaCl solution (154 mM) for an additional 30 min fixation. The gregarines were washed with distilled water, dehydrated with a graded series of ethyl alcohol, and critical point dried with CO_2. Filters were mounted on stubs, sputter coated with 5 nm platinum, and viewed under a Hitachi S-4300 scanning electron microscope (Hitachi, Tokyo, Japan).

2.3. DNA extraction and sequencing

Around 20 trophozoites of each species were isolated from the dissected hosts, washed three times in 154 mM physiological NaCl solution and deposited into a 1.5-ml microcentrifuge tube. DNA extraction was performed using the Qiagen DNeasy Blood & Tissue extraction kit. Small subunit rDNA sequences were PCR-amplified using a total volume of 25 μl containing 1.5 μl of primers, 1.5 μl of DNA template, 22 μl of ultra-pure water and a puReTaq Ready-to-go PCR bead (GE Healthcare, Quebec, Canada). The SSU rDNA sequences for *C. conus* n. sp. were amplified in three fragments using universal eukaryotic PCR primers: 525F 5′-AAG TCT GGT GCC AGC AGC C-3′ and R4 5′-GAT CCT TCT GCA GGT TCA CCT AC-3′, 917FD 5′-GCC AGA GGT GAA ATT CTN GG-3′ and R4 5′-GAT CCT TCT GCA GGT TCA CCT AC-3′, NPF1 5′-TGC GCT ACC TGG TTG ATC C-3′ and 1050MRD 5′-GCC TYG CGA CCA TAC TCC-3′. For *H. longissima*, custom primers Helio-29F 5′-CAT GCA TGT GTT CGG CAC TT-3′ and Helio-637R 5′-ACT CGC GGA GGA AAT GTC AA-3′ were developed and used based on existing *H. longissima* SSU rDNA sequences. A PCR was performed using a Thermal Cycler (Bio-Rad) with Lid set at 100 °C. The protocol included four cycles of an initial denaturation step at 94 °C for 4.5 min, 45 °C for 1 min and 72 °C for 1.45 min, followed by 34 cycles of 94 °C for 30 sec (denaturation), 50 °C for 1 min (annealing), 72 °C for 1.45 min (extension), with a final extension period at 72 °C for 10 min. PCR products for *C. conus* and *H. longissima* corresponding to the expected size were gel isolated using the GeneJET Gel Extraction Kit (Thermo Scientific). The cleaned PCR product for *H. longissima* was sent for sequencing. The PCR product for *C. conus* was cloned into the vector using the StrataClone PCR Cloning kit (Agilent). PCR products were digested with EcoRI and screened for size. Clones were sequenced using vector primers. Two SSU rDNA clones were sequenced from *C. conus*. The SSU rDNA sequence from *C. gammari* was extracted from a transcriptomic data set generated in the umbrella project 'Developing gregarine apicomplexans as aquatic symbiosis model system'. These transcriptome data have not been published yet. The new SSU rDNA sequences were initially identified by BLAST analysis and subsequently verified with molecular phylogenetic analyses. SSU rDNA data for *C. conus* (1817 bp), *C. gammari* (1890 bp), and *H. longissima* (271 bp, 5′-end) were uploaded to GenBank, Accession numbers PP326845, PP326846 and PP656908, respectively.

2.4. Molecular phylogenetic analysis

The three new SSU rDNA sequences were MAFFT ver. 7.490 (Katoh and Standley, 2013; Katoh et al., 2002) aligned with 47 other SSU rDNA sequences chosen based on closely related results from Nucleotide BLAST (GenBank) to represent gregarines with *Cryptosporidium* species as the outgroup. The model for the phylogenetic tree was selected using MEGA ver. 11.0.13 (Tamura et al., 2021). A maximum likelihood (ML) tree based on the 50-taxon dataset (1738 bp) was generated using RAxML ver. 8.2.11 (Stamatakis, 2014) under the general time-reversible (GTR) model of base substitutions that incorporated invariable sites and a discrete gamma distribution with eight rate categories. ML bootstrap analyses were conducted with

1000 pseudoreplicates and one heuristic search per pseudoreplicate. Bayesian analysis was conducted on the same dataset using MrBayes ver. 3.2.6 (Huelsenbeck and Ronquist, 2001) under the GTR model with four gamma rate categories. The chain heating coefficient (temp) was set to 0.2. The inference was conducted using four independent runs of four MCMC, each including 10 million generations. The relative burn-in fraction was set to 50 %. Posterior probabilities reflect the frequency at which a specific node was present in the post burn-in trees. A pair-wise distance calculation based on Kimura's two-parameter model (Kimura, 1980) was performed on a subset of the alignment using MEGA ver. 11.0.13 (Tamura et al., 2021). Parameters for the calculation were set as follows: pairwise deletion, 10,000 bootstraps, substitutions with transitions and transversions, gamma distributed rates among sites, and a gamma parameter at 4.0.

2.5. Statistical analysis

Prevalences of each gregarine species were calculated for every sampling date and overall for each month. Prevalence along with Clopper-Pearson 95 % confidence intervals were reported. Host body weight was compared between specimens infected with a single gregarine species rather than concurrent infections. Results are presented in box plots. Statistical analyses were conducted using Microsoft Excel and R ver. 4.2.2 (R Core Team, 2022). Significance was set at $p \leq 0.05$.

2.6. ZooBank registration

This article was registered in the Official Register of Zoological Nomenclature (ZooBank) as: urn:lsid:zoobank.org:pub:191D15E2-AC54-4E45-B755-42BACA84E6E2.

3. Results

3.1. Morphological observations

Heliospora longissima trophozoites were long and thin with a clearly visible nucleus in the centre of the deutomerite. The deutomerite was long and thin with a short protomerite. The trophozoites were on average 93 µm (69–170 µm, $n = 100$) long and 9 µm (7–16 µm, $n = 100$) wide (Fig. 1).

Cephaloidophora gammari trophozoites were observed to have a short and round deutomerite and protomerite, with the nucleus positioned off-centre towards the posterior end of the deutomerite (Fig. 2A). The trophozoite was found to be on average 48 µm (37–59 µm, $n = 100$) long and 29 µm (19–39 µm, $n = 100$) wide (Fig. 1). The epimerite

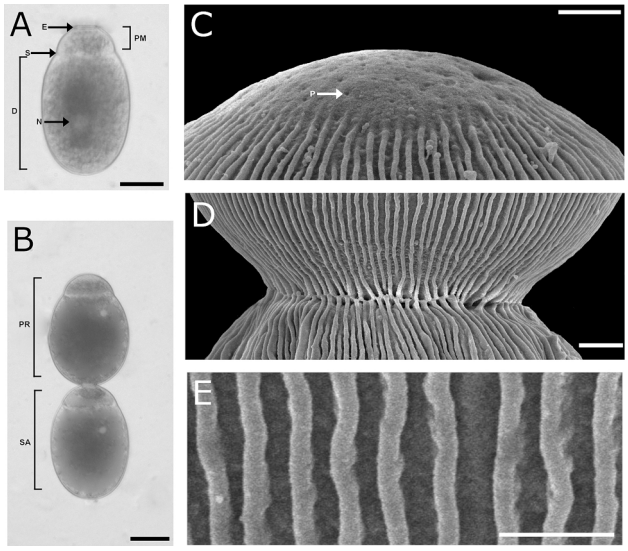

Fig. 2. Light micrographs and scanning electron micrographs (SEM), showing the general morphology and surface ultrastructure of the gregarine *Cephaloidophora gammari*. (**A**) A trophozoite showing the cell organization of the gregarine. The cell is divided by a septum (S) into the protomerite (PM) with the epimerite (E) at the anterior end and the deutomerite (D) with the spherical nucleus (N). (**B**) An association of two gregarines paired up in caudo-frontal syzygy. The anterior trophozoite is the primite (PR), while the posterior trophozoite is the satellite (SA). (**C**) Higher magnification SEM of the anterior end of a trophozoite with the epimerite free of epicytic folds. There is a visible separation between the protomerite with folds and the epimerite without folds. Surface pores (P) are distributed across the epimerite. (**D**) Higher magnification SEM of the junction between primite and satellite. (**E**) High magnification SEM of the epicytic folds. Scale bars: 500 nm (E), 1 µm (C, D), and 15 µm (A, B).

contained an even distribution of surface pores with no distinct pattern visible in SEM micrographs (Fig. 2C). Gamonts pair up in caudo-frontal syzygy in which the anterior gregarine is called the primite and the posterior gregarine is called the satellite (Fig. 2B). There was no obvious pattern of the satellite being conspicuously smaller or bigger than the primite. SEM micrographs demonstrated that the protomerite and the deutomerite were continuously covered in epicytic folds. The density of folds were 5 folds/µm (Fig. 2E). Single trophozoites and two individuals in syzygy were capable of gliding movements. There was a visible junction between the primite and the satellite of associated gamonts. In the junction the folds of the primite and satellite showed an alternating pattern (Fig. 2D).

Cephaloidophora conus n. sp. was named due to its more cone-

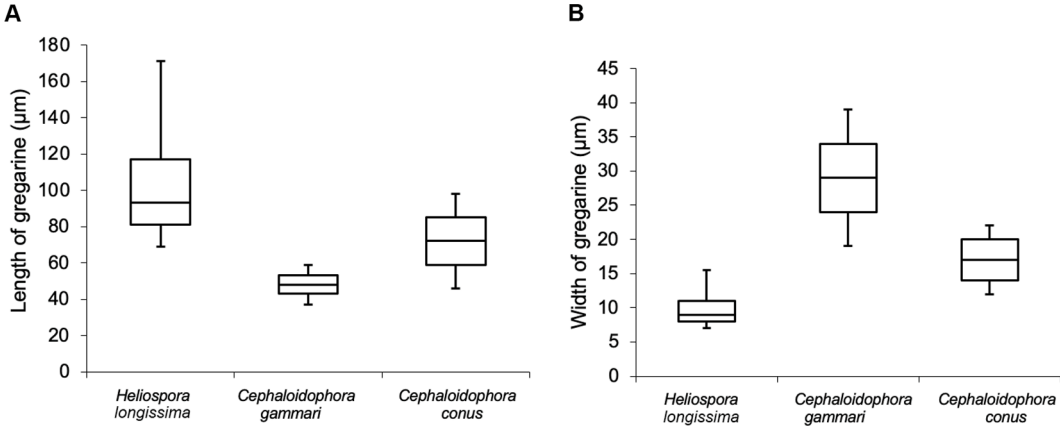

Fig. 1. Average length (A) and width (B) of gregarine species collected in the current study based on a sample population size of 100 individuals per species. Length is measured from the end of deutomerite to the tip of the protomerite. Width is measured across the centre of the deutomerite. All measurements in µm.

shaped appearance compared to the other gregarine symbionts found in *G. pulex*. *Cephaloidophora conus* has a longer and thinner deutomerite compared to *C. gammari*, with a nucleus centrally located towards the protomerite. The protomerite was observed to be round and protrudes from the deutomerite at the septum (Fig. 3A). *Cephaloidophora conus* trophozoites were measured at a length of around 72 μm (46–98 μm, $n = 100$) and a width of around 17 μm (12–22 μm, $n = 100$) (Fig. 1). The septum was clearly visible with light microscopy (Fig. 3A, B). Gamonts pair up in caudo-frontal syzygy (Fig. 3B). SEM micrographs demonstrated that the protomerite and the deutomerite were continuously covered in epicytic folds with a slight indentation at the level of the septum. The density of folds was up to 5 folds/μm. Single trophozoites and two individuals in syzygy were capable of gliding movements.

3.2. Molecular phylogenetic analysis

Phylogenetic analyses of the 50-taxon dataset resulted in a strongly supported clade of cryptosporidians (outgroup), one strongly supported terrestrial gregarine clade, a second strongly supported terrestrial clade as sister group to the aquatic eugregarines, and a poorly supported backbone for the aquatic eugregarines and archigregarines (Fig. 4). Aquatic eugregarines formed a clade consisting of the genera *Pterospora*, *Lithocystis*, *Lankesteria*, and *Lecudina* found in polychaetes, tunicates, etc. The obtained sequences from *Cephaloidophora* and *Heliospora* formed a strongly supported clade within the aquatic eugregarines (Fig. 4) and sister group to *Porospora*. This clade consisted of eugregarines isolated from the intestines of marine and freshwater crustaceans (*Cephaloidophora*, *Heliospora*, *Thiriotia*, and *Ganymedes*). They formed two sister clades, *Cephaloidophora* grouped with *Thiriotia* and *Heliospora* with *Ganymedes*. All gregarine sequences from crustaceans formed a weakly supported clade with *Lecudina polymorpha* (Fig. 4). Aquatic eugregarines formed a weekly supported clade with the archigregarines (*Selenidium* spp.). *Trichotokara* species branched directly off the archigregarine clade.

Sequence divergence in the crustacean clade made up of 10 sequences ranged from 0.3 % to 33.5 % (Table 1). The sequences of the *Cephaloidophora* species differed between 6.7 % and 17.6 %, while the difference between the *Heliospora* sequences ranged from 0.3 % to 6.6 %.

3.3. Prevalence of infection

The numbers of collected *G. pulex* varied over the year, with the highest number of *G. pulex* being caught in May 2021 and June 2021 (with an average of 82 and 87, respectively) and the lowest number being caught in December 2020 and December 2021 (an average of 17 and 8, respectively).

Gregarines occurred in *G. pulex* across the sampling period with the highest prevalence increase in spring and autumn, reaching the value of 46 % in November 2020, 45 % in April 2021, and 45 % in November 2021 (Fig. 5). The minimum share of infected *G. pulex* was recorded in July 2021 and August 2021 (17 % and 19 %, respectively). *Cephaloidophora gammari* and *C. conus* n. sp. showed similar infection patterns with a prevalence peak of 46 % in November 2020 (Fig. 6). *Heliospora longissima* infection peaked during April 2021 with a prevalence of 45 % (Fig. 6) opposite to the two *Cephaloidophora* species. *Cephaloidophora gammari* prevalence was lowest in April 2021, coinciding with the peak prevalence of *H. longissima* (Fig. 6). Concurrent infections had an overall prevalence of 19.5 % throughout the entire sampling period. *Heliospora longissima* prevalence was lowest in the summer (July 2021) when mean host size was smallest (3.6 ± 2 mg) (Fig. 7). Mean infected *G. pulex* wet weight was 11.7 ± 2.3 mg. The mean weight of *G. pulex* with single species infections of the observed gregarines differed. *Gammarus pulex* infected with *H. longissima* weighed 20.5 ± 0.9 mg ($n = 100$), with *C. gammari* 8.7 ± 1.9 mg ($n = 100$), and with *C. conus* 10.9 ± 1.1 mg ($n = 100$) (Fig. 8).

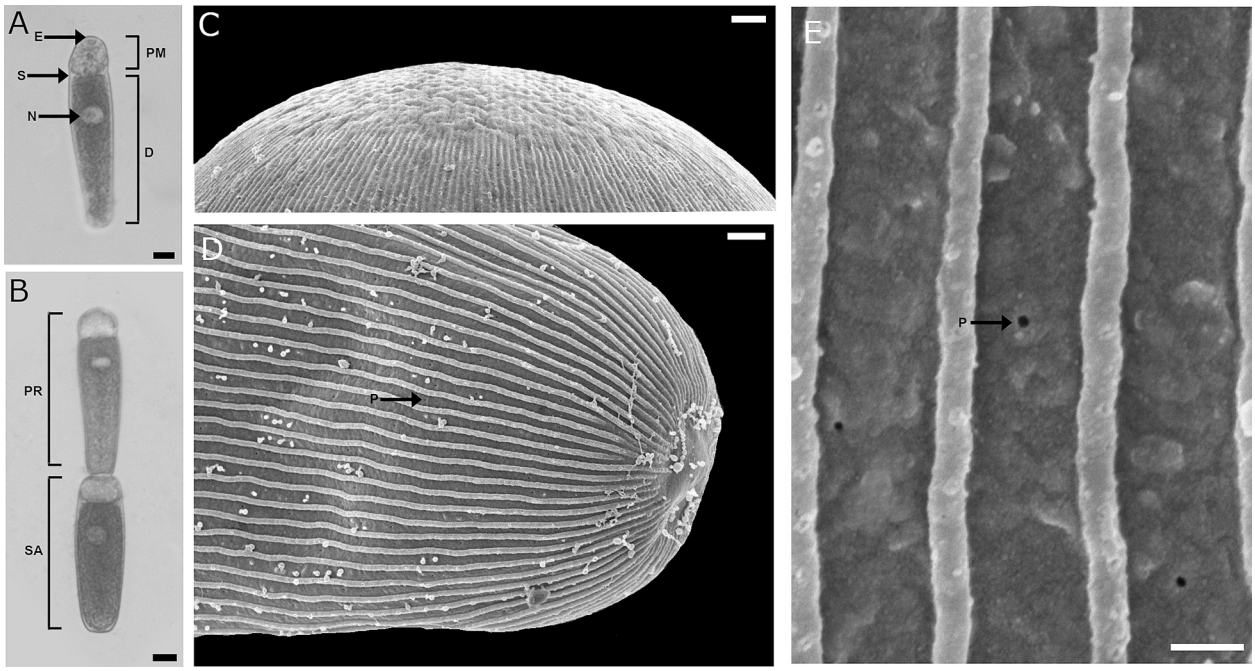

Fig. 3. Light micrographs and scanning electron micrographs (SEM), showing the general morphology and surface ultrastructure of the gregarine *Cephaloidophora conus* n. sp. (**A**) A trophozoite showing the cell organization of the gregarine. The cell is divided by a septum (S) into the protomerite (PM) with the epimerite (E) at the anterior end and the deutomerite (D) with the spherical nucleus (N). (**B**) An association of two gregarines paired up in caudo-frontal syzygy. The anterior trophozoite is the primite (PR), while the posterior trophozoite is the satellite (SA). (**C**) Higher magnification SEM of the anterior end of a trophozoite with the epimerite. There is a visible junction between the protomerite and the epimerite. (**D**) Higher magnification SEM of the posterior end of the trophozoite. Arrow denotes a surface pore (P). (**E**) High magnification SEM of the epicytic folds. The density of the folds is up to 5 folds/μm. Arrow denotes a pore (P). Scale bars: 250 nm (E), 1 μm (C, D), and 10 μm (A, B).

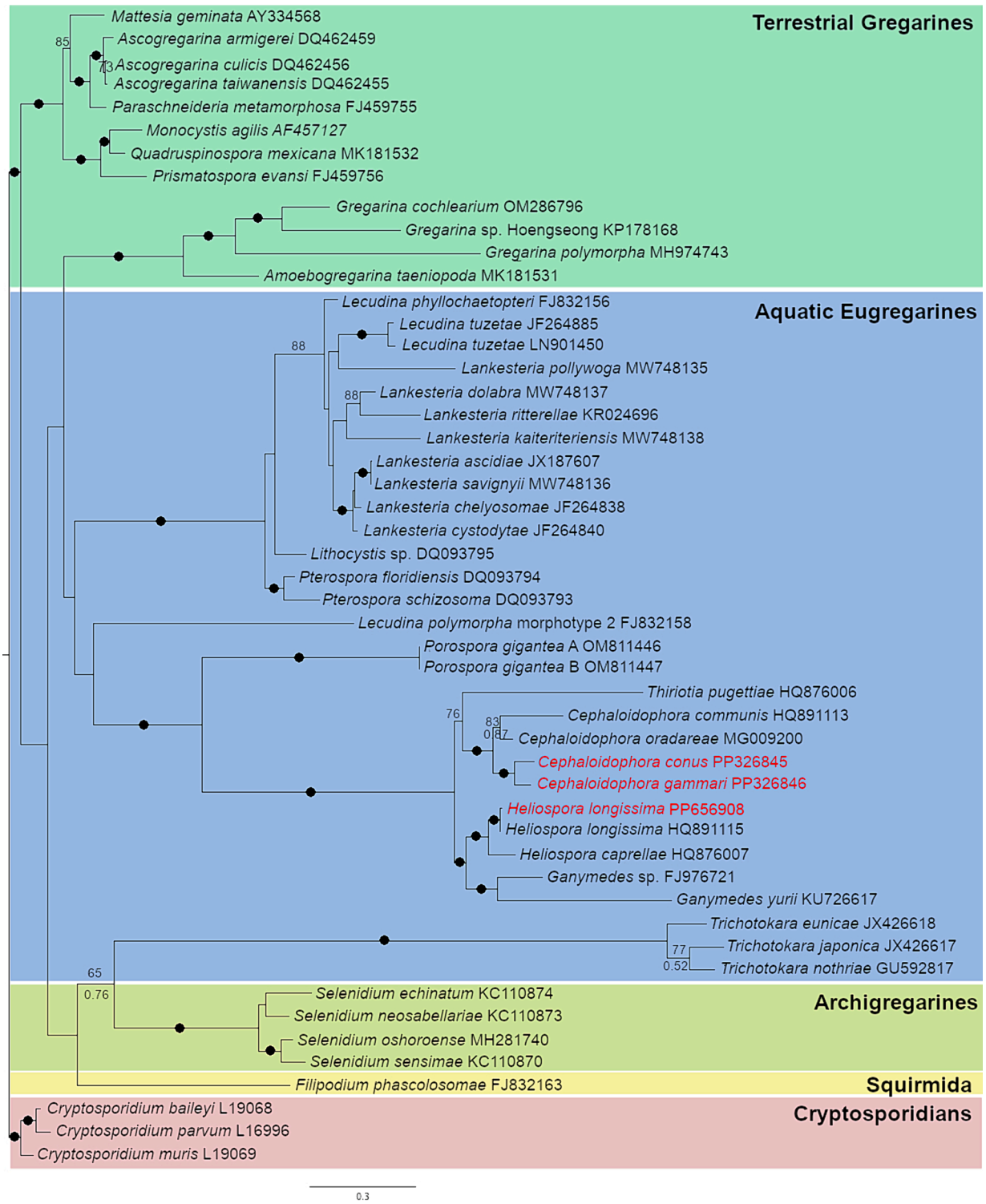

Fig. 4. Maximum likelihood (ML) tree of apicomplexans inferred using the GTR model of substitution on an alignment of 50 small subunit (SSU) rDNA sequences (1738 bp). Numbers at the branches denote bootstrap percentage (top) and Bayesian posterior probabilities (bottom). Black dots on branches denote Bayesian posterior probabilities and bootstrap percentages of 90 % or higher. Bootstrap values/posterior probabilities lower than 50/0.5 are not shown.

4. Discussion

In this study we identified three gregarine species infecting *G. pulex* in the Water of Leith river, Scotland, UK. These were the previously described *H. longissima* and *C. gammari*, plus the newly described *C. conus* (ex. *Cephaloidophora* sp.).

The size of the trophozoites of *H. longissima* in this study were smaller, but in the range of the measurements provided by Rueckert et al. (2011) and Goodrich (1949) (Table 2). Similarly, measurements of *C. gammari* in the current study agreed with that reported by Goodrich (1949). Initially Wróblewski et al. (2019) identified a gregarine species found in *G. pulex* as *Cephaloidophora* sp. based solely on morphological characteristics. There was uncertainty whether these specimens represented a life stage of *C. gammari* or a distinct species. Morphologically it

Table 1
Pairwise genetic distances in % calculated under the Kimura-2-parameter model. Newly generated sequences are marked in bold.

Sequence	1	2	3	4	5	6	7	8	9	10
1. *C. communis* (HQ891113)	–	–	–	–	–	–	–	–	–	–
2. ***C. conus* n. sp. (PP326845)**	**17.6**	–	–	–	–	–	–	–	–	–
3. *C. oradareae* (MG009200)	12.2	11	–	–	–	–	–	–	–	–
4. ***C. gammari* (PP326846)**	**17.3**	**6.7**	**10.9**	–	–	–	–	–	–	–
5. *Ganymedes* sp. (FJ976721)	21.8	24.3	18.8	24.4	–	–	–	–	–	–
6. *H. caprellae* (HQ876007)	20.1	18.7	15.3	19	17	–	–	–	–	–
7. ***H. longissima* (PP656908)**	**21.6**	**14.8**	**14.7**	**15.7**	**14.6**	**6.6**	–	–	–	–
8. *H. longissima* (HQ891115)	19.3	19.2	14.9	19.4	16.4	6.1	0.3	–	–	–
9. *T. pugettiae* (HQ876006)	27	28.4	24.2	28.5	25.4	24.4	33.3	24.1	–	–
10. *G. vurii* (KU726617)	30.5	32.9	27.7	33.5	25.4	27.7	28.4	26.7	30.7	–

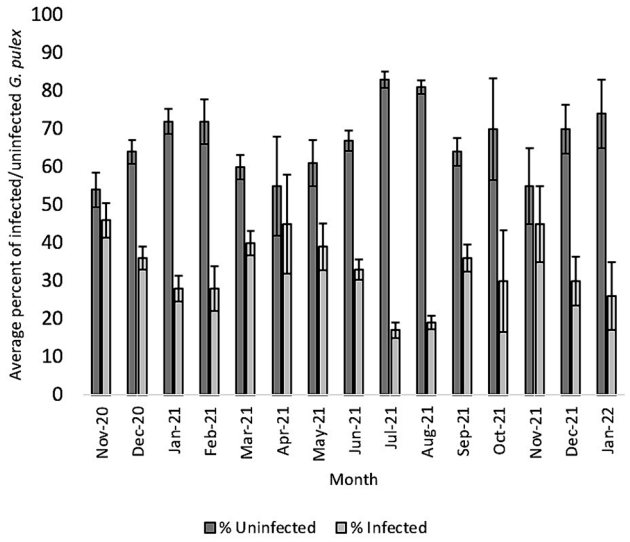

Fig. 5. Seasonal difference in average percent of infected and uninfected *Gammarus pulex* collected during 2-hr sampling trips in the Water of Leith river in Scotland. Error bars represent Clopper-Pearson 95% confidence interval.

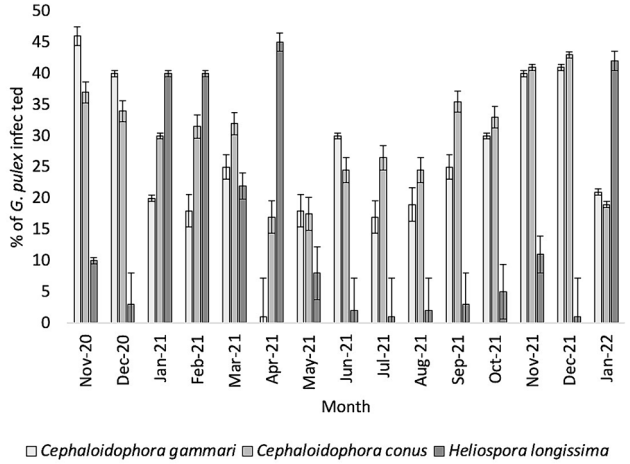

Fig. 6. Prevalence of gregarine infections in the amphipod *Gammarus pulex* over the sampling period in the Water of Leith. Error bars represent Clopper-Pearson 95% confidence interval.

falls between *C. oradareae* and *C. communis* (Table 2). However, in the current study, the sequencing results have unequivocally established its taxonomic position, confirming it as a separate species, which we describe here as *C. conus*. Molecular phylogenetic analyses have shown that it belongs to the *Cephaloidophora* genus and it is closely related to *C. gammari* (Fig. 4). Sequence divergence between those two sequences

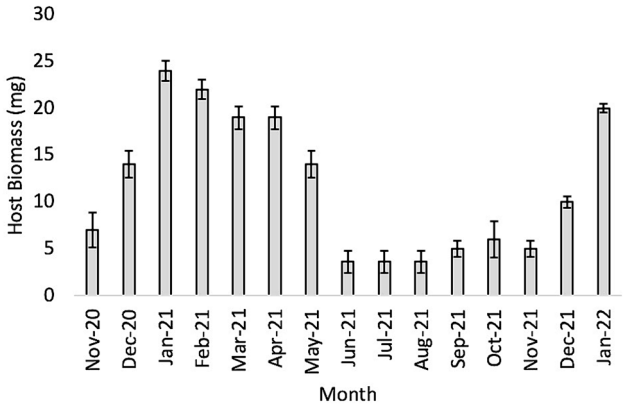

Fig. 7. Average infected *Gammarus pulex* body weight (mg) collected in each sampling trip across the 1-year sampling period. Error bars represent Clopper-Pearson 95% confidence interval.

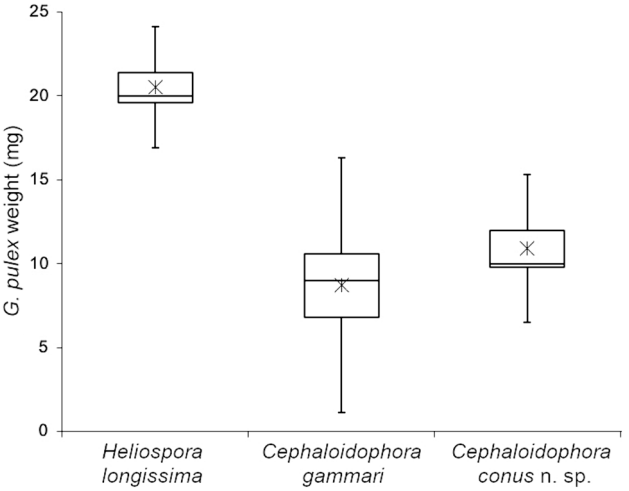

Fig. 8. Differences in *Gammarus pulex* body weight (mg) when infected with only one of the three gregarine species *H. longissima*, *C. gammari,* or *C. conus* n. sp. (100 infected *Gammarus* measured for each gregarine species).

was 6.7 % (Table 1), supporting the establishment of a new species. *Cephaloidophora oradareae* and *C. communis* form a separate clade in the phyologenetic trees. The designated species, *H. longissima* HQ891115 (Fig. 4), was documented in two amphipod species (*Eulimnogammarus verrucosus* and *E. vittatus*) taken from Lake Baikal, Russia (Rueckert et al., 2011). We encountered *H. longissima* in the amphipod *G. pulex*, taken from the Water of Leith river in Scotland, UK. Despite the different host species and sample locations, the genetic sequences derived from *H. longissima* exhibited only a 0.3 % difference (Table 1).

While some gregarines have been observed to be host-specific (Patil

Table 2
Comparison of morphological characteristics observed in gregarine species infecting *Gammarus* and closely related species.

	Heliospora longissima	*Cephaloidophora gammari*	*Cephaloidophora communis*	*Cephaloidophora oradareae*	*Cephaloidophora conus*
Host	*Gammarus pulex* *Orchestia littorea* *Gammarus roeselii* *Gammarus fasciatus* *Gammarus balcanicus* *Eulimnogammarus verrucosus* *Eulimnogammarus vittatus* *Caprella aequilibra* *Dikerogammarus villosus*	*Gammarus pulex* *Gammarus fasciatus*	*Balanus amphitrite* *Balanus eburneus* *Balanus crenatus* *Balanus glandula* *Balanus cariosus* *Balanus improvisus*	*Oradarea* sp.	*Gammarus pulex*
Cell shape	Trophozoites long and slender, epimerite showed prominent collar-like margin under SEM, protomerite short and rounded, septum clearly visible under LM and SEM, deutomerite long and slender	Short and round deutomerite and protomerite	Cylindrical in shape, epimerite rudimental and rounded, deutomerite longer than protomerite, septum clearly visible under LM	Cylindrical and rigid, protomerite and deutomerite were divided by a distinct septum	Longer and thinner deutomerite than *C. gammari*, protomerite round and protrudes from the deutomerite at the septum, septum clearly visible under LM
Length	93 μm (69–170 μm, $n = 100$)[1] 154 μm (57.9–273 μm, $n = 16$)[2]	48 μm (37–59 μm, $n = 100$)[1]	46.7 μm (24.3–80 μm, $n = 24$)[2]	40 μm (34–48 μm, $n = 20$)[3]	72 μm (46–98 μm, $n = 100$)[1]
Width	9 μm (7–16 μm, $n = 100$)[1] 17 μm (9.6–25 μm, $n = 16$)[2]	29 μm (19–39 μm, $n = 100$)[1]	17.8 μm (8.3–33 μm, $n = 24$)[2]	13 μm (11–15 μm, $n = 20$)[3]	17 μm (12–22 μm, $n = 100$)[1]
Longitudinal folds	3 folds/μm	5 folds/μm	6 folds/μm	4 folds/μm	5 folds/μm
Nucleus position	Situated in the middle of the deutomerite or slightly shifted to the anterior end	Off-centre towards the posterior end of the deutomerite	Middle of the deutomerite or sometimes shifted toward either the posterior or anterior end	Located in the upper portion of the deutomerite	Centrally located towards the protomerite

[1] Current study, [2]Rueckert et al. (2011), [3]Wakeman et al. (2018).

et al., 1985; Walsh and Olson, 1976; Wise et al., 2000), this is not the case for neither *H. longissima* nor *Cephaloidophora* spp. *Heliospora longissima* is a widespread gregarine species which has previously been described to infect *G. pulex* in France, Germany, and Poland (Wróblewski et al., 2019). It has also been found to infect *Orchestia littorea* and *Caprella aequilibra* in France; *Gammarus roeselii* in Germany; *Gammarus balcanicus* in Romania, *Dikerogammarus villosus* in Poland (Bojko et al., 2019; Codreanu-Bălcescu, 1996; Ovcharenko et al., 2009); and *Eulimnogammarus verrucosus* and *Eulimnogammarus vittatus* in Siberia, Russia (Rueckert et al., 2011). Members of the genus *Cephaloidophora* have been identified in a diverse range of hosts, including cirripedes, decapods, and amphipods. *Cephaloidophora gammari* infects freshwater gammaroids, particularly the amphipod *G. pulex*. This gregarine has been identified to infect *G. pulex* in several different countries, including the United Kingdom, France, Switzerland, Slovenia, Slovakia, Poland, and in the South Baltic coastal stream (Narasimhamurti, 1964; Wróblewski et al., 2019).

A survey of *G. pulex* in the Water of Leith, Scotland revealed distinct patterns of infection with the three gregarine species (*H. longissima*, *C. gammari*, and *C. conus*). While the occurrence of *H. longissima* and *C. gammari* can vary significantly depending on factors such as the host species, geographic location, and environmental conditions, infections of these two species seem to have no discernible impact on the population size, as has been previously shown for the amphipod *Gammarus fasciatus* (Grunberg and Sukhdeo, 2017). Herein, the most significant surge in gregarine infections was evident during the spring and autumn seasons, reaching up to 46 % in November (Fig. 5). Conversely, the lowest infection rates were recorded in July and August, standing at 17 % and 19 %, respectively. Wróblewski et al. (2019) also noted the highest prevalence increases for *H. longissima*, *C. gammari*, and *Cephaloidophora* sp. (now *C. conus*) in *G. pulex* in early spring, with the lowest prevalence rates in July. *Cephaloidophora gammari* and *C. conus* primarily infected *G. pulex* during November, while *H. longissima* showed a propensity to infect hosts in April (Fig. 6). These findings align with those of Grunberg and Sukhdeo (2017), who observed that *C. gammari* reaches its peak prevalence during the autumn months, while *H. longissima* peaks in the spring. Each of the gregarine species examined in our study displayed an annual peak in prevalence followed by a noticeable decline. These seasonal infection patterns observed in our study may be attributed to the development of gametocysts, a process highly influenced by temperature and humidity levels. Notably, *C. gammari* exhibited its lowest prevalence in April, coinciding with the peak prevalence of *H. longissima* (Fig. 6). The prevalence of *H. longissima* correlated with the size of *G. pulex* (Fig. 4). Its prevalence was lowest in the summer when mean *G. pulex* host size was the smallest (3.6 ± 2 mg) (Figs. 3, 4). Grunberg and Sukhdeo (2017) reported similar observations for the prevalence of *H. longissima*, which increased with the increasing size of the host *G. fasciatus*. Grunberg and Sukhdeo (2017) suggested this could be due to the size and morphology of *H. longissima* oocysts which are larger than the oocysts of *C. gammari* at around 8 μm in diameter, with additional ~ 10 μm long ray-like processes extending from the cyst, while *C. gammari* oocysts are smaller at around 5 μm with no processes (Goodrich, 1949).

Understanding the factors that influence gregarine occurrence and prevalence is important as they can significantly impact the health and behaviour of their hosts (Field and Michiels, 2006; Marden and Cobb, 2004). They can reduce the host's lifespan, lead to host mortality (Field and Michiels, 2006), or they may alter the host's behaviour in ways that benefit the symbiont, for instance, infected insects that spend more time feeding, increase the chance of gregarine transmission to other hosts via the faecal-oral route (De Bekker et al., 2018). As *G. pulex* is an important invertebrate species in the food web and ecology of freshwater ecosystems, it is essential to understand how this freshwater shrimp is coping with possible infections/colonizations. In this study, we are taking a step towards understanding the relationship of *G. pulex* with its gregarine species.

5. Conclusion

Future work should focus on studying if the three gregarine species have a significant impact on the health and/or behaviour of their hosts. Gregarines are also important from an ecological perspective (Bojko

et al., 2019), as they may play a role in regulating host populations by reducing the reproductive success of infected individuals or making them more vulnerable to other predators or environmental stressors (Marden and Cobb, 2004). Understanding the factors that influence infection/colonization patterns could help to guide general management efforts aimed at protecting freshwater ecosystems.

6. Taxonomic summary

Superphylum Alveolata Cavalier-Smith, 1991
Phylum Apicomplexa Levine, 1980, emend. Adl et al., 2005
Class Conoidasida Levine, 1988
Subclass Gregarinasina Dufour, 1828
Order Eugregarinorida Léger, 1900
Family Cephaloidophoridae Kamm, 1922

Cephaloidophora conus n. sp.

ZooBank registration number of the new species. urn:lsid:zoobank.org:act:DECF2747-4238-45CA-AAAD-048A17E82199.

Diagnosis. Deutomerites in *C. conus* are elongated and slender compared to those in *C. gammari*, featuring a centrally located nucleus towards the protomerite. The protomerite exhibits a rounded shape, extending outward from the deutomerite at the septum. Trophozoites of *C. conus* were measured at 72 μm in length (with a range of 46–98 μm, $n = 100$) and 17 μm in width (with a range of 12–22 μm, $n = 100$). The septum was clearly discernible under light microscopy. Gamonts form pairs in caudo-frontal syzygy. Scanning electron microscopy images revealed that both the protomerite and deutomerite were consistently covered in epicytic folds, displaying a slight indentation at the septum level. The density of folds reached up to 5 folds/μm. Individual trophozoites and paired individuals in syzygy exhibited gliding movements.

DNA sequence. Small subunit rDNA sequence has been deposited in GenBank under accession number PP326845.

Holotype. The name-bearing type of this species is the specimen illustrated in Figure 3A (Article 73.1.4 of the ICZN, 1999).

Type locality. Water of Leith, Scotland, UK (55°89′60.1″N, –3°30′77.9″W).

Type host. *Gammarus pulex* (Linnaeus, 1758) (Ampipoda: Gammaridae).

Site of infection. Intestine.

Etymology. The species name *conus* refers to the cone-shaped morphology of this species in comparison to the other gregarine species known to parasitize the host *Gammarus pulex*.

CRediT authorship contribution statement

Kevin McKinley: Writing – original draft, Investigation, Formal analysis. **Anastasios D. Tsaousis:** Writing – review & editing, Supervision, Funding acquisition, Conceptualization. **Sonja Rückert:** Writing – review & editing, Validation, Supervision, Project administration, Funding acquisition, Conceptualization.

Declaration of Competing Interest

The authors declare that they have no known competing financial interests or personal relationships that could have appeared to influence the work reported in this paper.

Data availability

Data will be made available on request.

Acknowledgements

KM would like to thank Monika Wiśniewska for advice on the molecular analysis and KM, AT and SR would like to thank Martin Kolisko for help with the trancriptome dataset. Both are based at the Institute of Parasitology, Biology Centre, Czech Academy of Sciences, České Budějovice, Czech Republic.

Funding

This work was supported by the Gordon and Betty Moore Foundation (project number: GBMF9327, https://doi.org/10.37807/GBMF9327). We acknowledge support by the Open Access Publication Fund of the University of Duisburg-Essen.

References

Adamo, S.A., 2013. Parasites: evolution's neurobiologists. J. Exp. Biol. 216 (1), 3–10.
Bojko, J., Stentiford, G.D., Stebbing, P.D., Hassall, C., Deacon, A., Cargill, B., Pile, B., Dunn, A.M., 2019. Pathogens of *Dikerogammarus haemobaphes* regulate host activity and survival, but also threaten native amphipod populations in the UK. Dis. Aquat. Org. 136 (1), 63–78.
Cheshmedjiev, S., Soufi, R., Vidinova, Y., Tyufekchieva, V., Yaneva, I., Uzunov, Y., Varadinova, E., 2011. Multi-habitat sampling method for benthic macroinvertebrate communities in different river types in Bulgaria. Water Res. Manag. 1 (3), 55–58.
Codreanu-Bălcescu, D., 1996. Sur les grégarines (Protozoa, Sporozoa) parasites chez *Rivulogammarus* (Crust., Amph.) des ruisseaux de montagne en Roumanie. [On the gregarines (Protozoa, Sporozoa) parasites in *Rivulogammarus* (Crust., Amph.) of mountain streams in Romania]. Rev. Roumaine de Biol Sér. Biol. Anim. 41, 7–15.
De Bekker, C., Will, I., Das, B., Adams, R.M., 2018. The ants (Hymenoptera: Formicidae) and their parasites: effects of parasitic manipulations and host responses on ant behavioral ecology. Myrmecol. News 28, 1–2.
Diakin, A., Paskerova, G.G., Simdyanov, T.G., Aleoshin, V.V., Valigurová, A., 2016. Morphology and molecular phylogeny of coelomic gregarines (Apicomplexa) with different types of motility: *Urospora ovalis* and *U. travisiae* from the polychaete *Travisia forbesii*. Protist 167 (3), 279–301.
Field, S.G., Michiels, N.K., 2006. Does the acephaline gregarine *Monocystis* sp. modify the surface behaviour of its earthworm host *Lumbricus terrestris*? Soil Biol. Biochem. 38 (6), 1334–1339.
Frolova, E., Paskerova, G., Smirnov, A., Nassonova, E., 2021. Molecular phylogeny and new light microscopic data of *Metchnikovella spiralis* (Microsporidia: Metchnikovellidae), a hyperparasite of eugregaine *Polyrhabdina* sp. from the polychaete *Pygospio elegans*. Parasitology 148 (7), 779–786.
Goodrich, H.P., 1949. *Heliospora* n.g. and *Rotundula* n.g., gregarines of *Gammarus pulex*. Q. J. Microsc. Sci. 90 (1), 27–35.
Grabner, D., Sures, B., 2019. Amphipod parasites may bias results of ecotoxicological research. Dis. Aquat. Org. 136, 121–132.
Grunberg, R.L., Sukhdeo, M.V., 2017. Temporal community structure in two gregarines (*Rotundula gammari* and *Heliospora longissima*) co-infecting the amphipod *Gammarus fasciatus*. J. Parasitol. 103 (1), 6–13. https://doi.org/10.1645/16-47.
Harlıoğlu, M.M., Farhadi, A., 2018. Importance of *Gammarus* in aquaculture. Aquacult. Int. 26, 1327–1338.
Huelsenbeck, J.P., Ronquist, F., 2001. MRBAYES: Bayesian inference of phylogenetic trees. Bioinformatics 17 (8), 754–755. https://doi.org/10.1093/bioinformatics/17.8.754.
ICZN, 1999. International Code of Zoological Nomenclature, 4th edn. International Trust for Zoological Nomenclature, London.
Ilvonen, J.J., Kaunisto, K.M., Suhonen, J., 2018. Odonates, gregarines and water mites: why are the same host species infected by both parasites? Ecol. Entomol. 43 (5), 591–600.
Kamiya, T., O'Dwyer, K., Nakagawa, S., Poulin, R., 2014. What determines species richness of parasitic organisms? A meta-analysis across animal, plant and fungal hosts. Biol. Rev. 89, 123–134.
Katoh, K., Standley, D.M., 2013. MAFFT multiple sequence alignment software version 7: improvements in performance and usability. Mol. Biol. Evol. 30 (4), 772–780. https://doi.org/10.1093/molbev/mst010.
Katoh, K., Misawa, K., Kuma, K., Miyata, T., 2002. MAFFT: a novel method for rapid multiple sequence alignment based on fast Fourier transform. Nucleic Acids Res. 30 (14), 3059–3066. https://doi.org/10.1093/nar/gkf436.
Kimura, M., 1980. A simple method for estimating evolutionary rates of base substitutions through comparative studies of nucleotide sequences. J. Mol. Evol. 16, 111–120.
Köprücü, K., Özdemir, Y., 2005. Apparent digestibility of selected feed ingredients for Nile tilapia (*Oreochromis niloticus*). Aquaculture 250, 308–316.
Macneil, C., Dick, J.T., Elwood, R.W., 1999. The dynamics of predation on *Gammarus* spp. (Crustacea: Amphipoda). Biol. Rev. 74, 375–395.
Marden, J.H., Cobb, J.R., 2004. Territorial and mating success of dragonflies that vary in muscle power output and presence of gregarine gut parasites. Animal Behav. 68 (4), 857–865.
Medina-Durán, J.H., Mayén-Estrada, R., Mariño-Pérez, R., Song, H., 2020. Morphology and phylogenetic position of two new gregarine species (Apicomplexa: Eugregarinorida) parasitizing the Lubber Grasshopper *Taeniopoda centurio* (Drury, 1770) (Insecta: Orthoptera: Romaleidae) in Mexico. J. Eukaryot. Microbiol. 67, 4–17.

Narasimhamurti, C., 1964. Observations on the gregarine *Rotundula gammari* (Diesing, 1859), Goodrich 1949. Parasitology 54 (1), 195–199.
Ovcharenko, M., Codreanu-Balcescu, D., Grabowski, M., Konopacka, A., Wita, I., Czaplinska, U., 2009. Gregarines (Apicomplexa) and microsporidians (Microsporidia) of native and invasive gammarids (Amphipoda, Gammaroidea), occurring in Poland. Wiad. Parazytol. 55 (2), 237–247.
Palmia, B., Bartoli, M., Laini, A., Bolpagni, R., Ferrari, C., Viaroli, P., 2019. Effects of drying and re-wetting on litter decomposition and nutrient recycling: a manipulative experiment. Water 11 (4), e708.
Patil, C.C., Amoji, S.D., Neelgund, Y.F., 1985. Studies on cross infection of cephaline gregarines of tenebrionid insects. Arch. Protistenk. 129, 179–182.
R Core Team, 2022. R: A language and environment for statistical computing. R Foundation for Statistical Computing, Vienna, Austria. https://www.R-project.org/ (accessed 30 November 2023).
Rueckert, S., Simdyanov, T.G., Aleoshin, V.V., Leander, B.S., 2011. Identification of a divergent environmental DNA sequence clade using the phylogeny of gregarine parasites (Apicomplexa) from crustacean hosts. PLoS One 6 (3), e18163.
Rueckert, S., Wakeman, K.C., Jenke-Kodama, H., Leander, B.S., 2015. Molecular systematics of marine gregarine apicomplexans from Pacific tunicates, with descriptions of five novel species of *Lankesteria*. Int. J. Syst. Evol. Microbiol. 65 (8), 2598–2614.
Rueckert, S., Betts, E.L., Tsaousis, A.D., 2019. The symbiotic spectrum: Where do the gregarines fit? Trends Parasitol. 35 (9), 687–694.
Rufchaei, R., Hoseinifar, S.H., Mirzajani, A., Van Doan, H., 2017. Dietary administration of *Pontogammarus maeoticus* extract affects immune responses, stress resistance, feed intake and growth performance of Caspian roach (*Rutilus caspicus*) fingerlings. Fish Shellfish Immunol. 63, 196–200.
Rynkiewicz, E.C., Pedersen, A.B., Fenton, A., 2015. An ecosystem approach to understanding and managing within-host parasite community dynamics. Trends Parasitol. 31, 212–221.
Schall, J.J., 2021. *Stomatocystis goerresi*, a new species of gregarine parasite (Apicomplexa, Monocystidae) from the invasive Japanese earthworm *Amynthas tokioensis* (Megascolecidae), with a description of the parasite's life cycle. Folia Parasitol. 68, 1–7.
Simdyanov, T.G., Guillou, L., Diakin, A.Y., Mikhailov, K.V., Schrével, J., Aleoshin, V.V., 2017. A new view on the morphology and phylogeny of eugregarines suggested by the evidence from the gregarine *Ancora sagittata* (Leuckart, 1860) Labbé, 1899 (Apicomplexa: Eugregarinida). PeerJ 5, e3354.
Sokolova, Y.Y., Paskerova, G.G., Rotari, Y.M., Nassonova, E.S., Smirnov, A.V., 2013. Fine structure of *Metchnikovella incurvata* Caullery and Mesnil 1914 (microsporidia), a hyperparasite of gregarines *Polyrhabdina* sp. from the polychaete *Pygospio elegans*. Parasitology 140 (7), 855–867.
Sorcetti, C.C., Di Giovanni, M.V., 1984. Gregarines (Protozoa-Sporozoa) in Italian freshwater arthropods. A Preliminary Contribution. Boll. Zool. 51 (3–4), 313–327.
Stamatakis, A., 2014. RAxML version 8: a tool for phylogenetic analysis and post-analysis of large phylogenies. Bioinformatics 30 (9), 1312–1313. https://doi.org/10.1093/bioinformatics/btu033.
Tamura, K., Stecher, G., Kumar, S., 2021. MEGA11: Molecular evolutionary genetics analysis version 11. Mol. Biol. Evol. 38 (7), 3022–3027. https://doi.org/10.1093/molbev/msab120.
Valigurová, A., Florent, I., 2021. Nutrient acquisition and attachment strategies in basal lineages: a tough nut to crack in the evolutionary puzzle of Apicomplexa. Microorganisms 9 (7), e1430.
Vigneron, A., Geffard, O., Coquery, M., François, A., Quéau, H., Chaumot, A., 2015. Evolution of cadmium tolerance and associated costs in a *Gammarus fossarum* population inhabiting a low-level contaminated stream. Ecotoxicology 24, 1239–1249.
Wakeman, K.C., Heintzelman, M.B., Leander, B.S., 2014. Comparative ultrastructure and molecular phylogeny of *Selenidium melongena* n. sp. and *S. terebellae* Ray 1930 demonstrate niche partitioning in marine gregarine parasites (Apicomplexa). Protist 165 (4), 493–511.
Walsh, R.D., Olson, J.K., 1976. Observations on the susceptibility of certain culicine mosquito species to infection by *Lankesteria culicis* (Ross). Mosq. News 36, 154–160.
Wise, M.R., Janovy, J., Wise, J.C., 2000. Host specificity in *Metamera sillasenorum*, n. sp., a gregarine parasite of the leech *Helobdella triserialis* with notes on transmission dynamics. J. Parasitol. 86, 602–606.
Wróblewski, P., Ovcharenko, M., Eichenlaub, J., Yuryshynets, V., 2019. Seasonality of microsporidian and gregarine parasitism in *Gammarus pulex* (Crustacea: Amphipoda) inhabiting the tributary of the Słupia river. Baltic Coastal Zone 23, 37–42.
Zamboni, D.S., Lima-Junior, D.S., 2015. Inflammasomes in host response to protozoan parasites. Immunol. Rev. 265, 156–171.